An apparent relation between ELM occurrence times and the prior phase evolution of divertor flux loop measurements in JET

S C Chapman[1,2,4], R O Dendy[3,1,4], A J Webster[2,3,4], N W Watkins[1,2], T N Todd[3,4], J Morris[3,4] and JET EFDA Contributors[4]

[1]*Centre for Fusion, Space and Astrophysics, Department of Physics, Warwick University, Coventry CV4 7AL, UK*

[2]*Max Planck Institute for the Physics of Complex Systems, Dresden, Germany*

[3]*CCFE, Culham Science Centre, Abingdon, Oxfordshire OX14 3DB, UK*

[4]*JET-EFDA, Culham Science Centre, Abingdon, Oxfordshire, OX14 3DB UK*

1. Introduction

Statistical and time domain analysis of ELMs in Joint European Torus (JET) plasmas is providing fresh insights into the ELMing process. These plasmas are often well adapted to such studies because of their long duration, such that large numbers of ELMs occur under quasi-stationary conditions. Understanding the ELMing process is a key challenge in magnetic confinement fusion plasma physics given the correlation between ELMing and enhanced confinement regimes, and the constraints on ELM magnitudes in future ITER plasmas. The ELMing process is a multiscale nonlinear plasma phenomenon and information on the underlying process can be acquired by analysing the distribution of events, here, ELM occurrences. This was noted initially in Refs.[1,2]. Subsequent advances in the scale and quality of the ELM data from JET, in particular, have led to rapid recent progress. Studies have involved: transitions in Type I ELMing in a sequence of similar JET plasmas in response to different gas puffing rates[3]; differentiating between Type I and Type III ELMs from first principles, in terms of extreme value distributions of inter-ELM time intervals[4]; and the identification of strong (and wholly unexpected) structure in the distribution of inter-ELM time intervals from a week-long sequence of quasi-identical JET plasmas[5]. Here we turn to a newly identified[6] correlation between ELM occurrence times in JET and the time evolution of a global measure of the plasma state. The latter is provided by the full flux loop VLD2 and VLD3 measurements, which are proportional to the changing poloidal magnetic flux through loops that encircle JET toroidally near the divertor coil system.

2. Results

We determine the ELM occurrence times t_N by identifying the peak of the Be II signal within each ELM as detailed in [6] and, from these, the intervals between successive ELMs Δt_N. Figure 1 plots the successive time intervals between one ELM and the next on a delay plot, that is, Δt_{N+1} versus Δt_N. There are gaps in the delay plot at time intervals where ELMs occur less often and the plot also shows that there is no ordering between the length of one

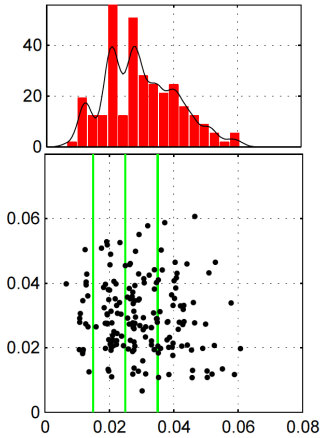

Fig.1: Statistics of inter-ELM time intervals Δt_N in JET plasma 83769. Top: probability density plotted as normalized histogram (red) with superimposed continuous pdf (black) inferred using kernel density estimation with a normal kernel with bandwidth of 0.002. Bottom: delay plot [3] of Δt_{N+1} versus Δt_N. Vertical green lines indicate $\Delta t = 0.015, 0.025, 0.035$.

inter-ELM interval and the next, that is, a short Δt_N can be followed by either a long or short Δt_{N+1}. From this plot we see that almost no ELMs occur within ~ 0.01 s of the preceding ELM and the most likely inter ELM time intervals are clustered within $\Delta t < 0.015; 0.015 < \Delta t < 0.025; 0.025 < \Delta t < 0.035$, for longer Δt clear gaps cannot be seen in this size of statistical sample. Figure 2 shows the VLD3 signal traces for all ELMs JET plasma 83769, corresponding to the first 3 groups of Fig.1. To afford comparison, the VLD3 traces have all been shifted in time such that t=0 is at the first minimum in the VLD3 signal following the first ELM, and in amplitude such that the trace is at zero at t=0. We have marked on these traces the occurrence times of the first (red) and second (green) ELMs. Ordering the data in this manner immediately suggests a clustering of ELM occurrence times with the phase of the VLD3 signal. The left hand panel shows that there is a population of prompt ELMs which can all be seen to arrive after about one-and-a-half to one-and-three-quarters oscillations of the VLD3 response to the previous ELM.

An instantaneous phase can be determined from the complex analytic signal as in [6]. In Figure 3 (left panel) we plot the instantaneous phase of the full flux loop signal versus time for all the ELMs in JET plasma 83769. We again need to choose a zero time from which to measure changes in the full flux loop phase following an ELM and we set this to be the time of the first ELM as determined from the Be II signal. We can see a clear phase bunching which we verified is found for *all* non-prompt ELMs in the flat-top period of H-mode in all these plasmas. The inter-ELM time intervals are not random: ELMs are more likely to occur when the full flux loop signals are at a specific phase w.r.t. that of the preceding ELM. This may explain the structure that can be seen in the inter-ELM time interval histograms, and which has been established in a larger statistical sample [5]. We now establish that this is not a trivial correlation. We generated a shuffled surrogate set of ELM arrival times from the data as follows. The surrogate occurrence time of an ELM is set as $t_N = t_{N-1} + \Delta t_j$ where the inter-

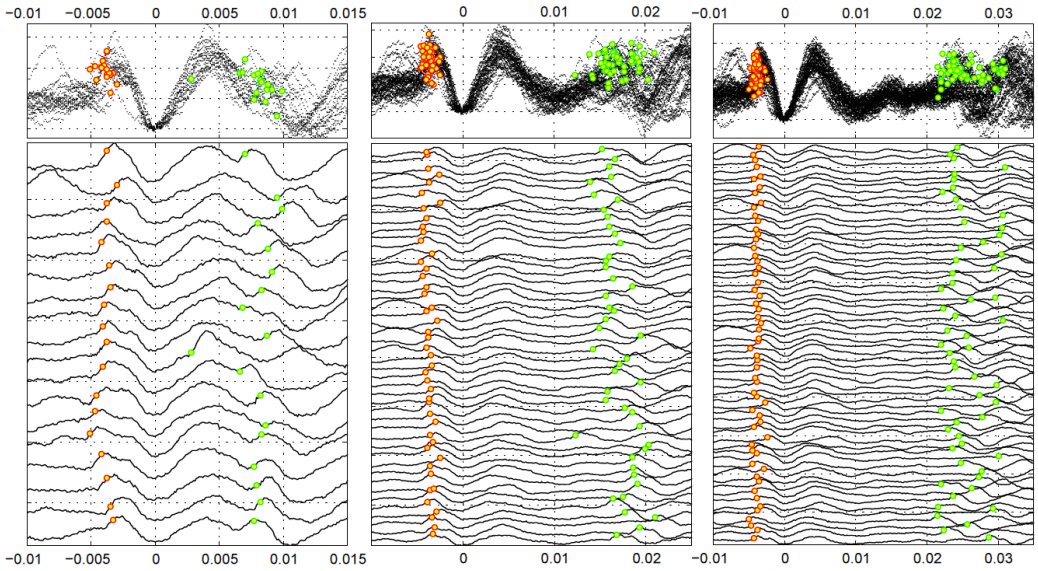

Fig 2: ELM occurrence times superimposed on VLD3 signal. Multiple time traces for different pairs of successive ELMs are displayed in three panels, corresponding to the first three groups of inter-ELM times indicated by red vertical lines in Fig.1. The three panels plot VLD3 signals (black dotted lines) for all ELMs for which the inter-ELM time interval is in the range: (left) $\Delta t < 0.015$ (centre) $0.015 < \Delta t < 0.025$ (right) $0.025 < \Delta t < 0.035$. These traces have all been shifted in time such that t=0 is at the first minimum in the VLD3 signal following the first ELM. Amplitude is set to zero at t=0. The VLD3 signal is normalized as in [6]. In the upper panels, the ELM times are marked on each VLD3 trace with yellow filled red circles (first ELM) and green circles (second ELM). The lower panels are a stack of the individual VLD3 signals, with ELM times denoted by red (first ELM) and green (second ELM) circles.

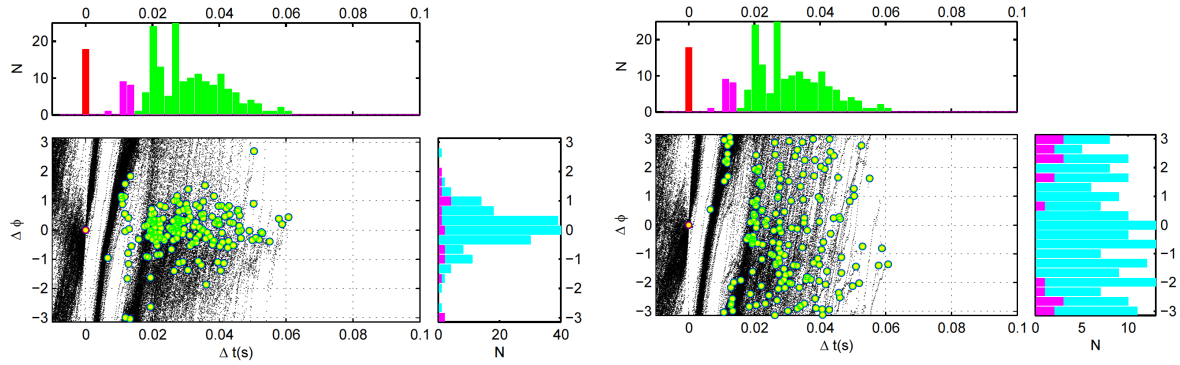

Fig 3: Left set of panels: ELM occurrence times and VLD3 phase difference between all pairs of ELMs in the flat-top of JET plasma 83769. Right set of panels: same format as left panel, but with randomly shuffled time order of the inter-ELM time intervals. Each set of panels is as follows. Main panel: VLD3 instantaneous phase, modulo 2π, plotted as a function of time, up to the occurrence time of the next ELM. The coordinates are time, and phase difference from the occurrence time of the first ELM. ELM occurrence times are marked on each VLD3 trace with yellow filled red circles (first ELM) and green circles (second ELM). Right hand panel: histogram of VLD3 phase difference at the time of the second ELMs, for inter-ELM time intervals $\Delta t < 0.015$ (magenta) and for all ELMs (cyan). Top Panel: histogram of inter-ELM time intervals.

ELM time interval Δt_j is now selected at random from the set of observed inter-ELM time intervals in the flat top of a given plasma. This preserves the set of inter-ELM times. Under this operation, the histogram of ELM arrival times shown in the preceding figures is unchanged. This is shown in Figure 3 (right panels), which is identical to the left panel

except that the sequence of ELM arrival times has been replaced with our surrogate. On this plot, we see that the statistical distribution of ELM arrival times is unchanged, but the phase bunching is completely lost.

3. Conclusions

In a series of steady-state H-mode plasmas in the Joint European Torus (JET), a phase relationship has been identified [6] between sequential ELM occurrence times and the phase of the signal of the changing poloidal magnetic flux in toroidal loops in the divertor region. We focused on ELMs observed in the Be II emission at the divertor, and compared inter-ELM time intervals with fluctuations of the signal in the full flux loops VLD2 and VLD3. Each ELM produces a clear response in the full flux loop signals, whose subsequent time evolution to the next ELM we study for several hundred pairs of ELMs. This time evolution is irregularly oscillatory, and a time dependent phase can be obtained by Hilbert transform. The arrival time of the second ELM in each pair is found [6] to fall into one of two categories: (1) prompt second ELMs, which are directly paced by the initial large-amplitude first cycle of the flux loop response to the first ELM; (2) later second ELMs, whose occurrence times are strongly bunched with respect to the phase difference of the flux loop signal from the time of the previous ELM. The full flux loop signals capture aspects of the global dynamics of the plasma, including large scale plasma motion and divertor dynamics. The quasistationary plasma state is maintained by perturbations from the control system reacting to plasma motion. Integrated over the large scale, the reaction of the plasma to these perturbations can be seen in the full flux loop signals. These signals reflect the control system and plasma behaving as a single nonlinearly coupled system, rather than as driver and response. Our result, that the instantaneous phase of the full flux loop signals is a predictor of ELM occurrence, may assist design of ELM mitigation strategies and help quantify their effectiveness. The prompt second ELMs have lower Be II peak amplitude. Insofar as peak Be II amplitude may correlate with ELM energy release, this suggests a possible ELM mitigation strategy of encouraging prompt ELM occurrence. We found one JET plasma where the prompt ELMs do not occur, suggesting that there may be plasma conditions that favour the occurrence of prompt ELMs that are intrinsic to JET operation.

This project has received funding from the European Union's Horizon 2020 research and innovation programme under grant agreement number 210130335 and from the RCUK Energy Programme [grant number EP/I501045]. The views and opinions expressed herein do not necessarily reflect those of the European Commission.

[1] A W Degeling, Y R Martin, P E Bak, J B Lister and X Llobet, Plasma Phys. Control. Fusion 43 1671 (2001)
[2] J Greenhough, S C Chapman, R O Dendy and D J Ward, Plasma Phys. Control. Fusion 45 747 (2003)
[3] F A Calderon, R O Dendy, S C Chapman, A J Webster, B Alper *et al*., Phys. Plasmas 20 042306 (2013)
[4] A J Webster and R O Dendy, Phys. Rev. Lett. 110 155004 (2013)
[5] A J Webster, R O Dendy, F A Calderon, S C Chapman, E Delabie, R Felton *et al*., Plasma Phys. Control. Fusion, 56 075017 (2014)
[6] S C Chapman, R O Dendy, T N Todd, N W Watkins, A J Webster, F A Calderon *et al*., Phys. Plasmas 21 062302 (2014)